Supporting Information

VanHouten et al. 10.1073/pnas.0911186107

SI Text

Immunofluorescent Staining and Surface Area (SA):Volume (V) measurement. Immunofluorescent staining for PMCA2 is detailed in ref. 1; immunostaining for phospho-STAT3, phospho-STAT5, and NFκB was performed using commercial protocols. Phospho-STAT3 (Tyr705, clone D3A7) and Phospho-STAT5 (Tyr 694, clone C11C5) antibodies were from Cell Signaling Technologies, and the NFκB (p50) antibody was from Santa Cruz Biotechnology. F-actin was stained with Alexa-488-phalloidin (Invitrogen). Staining was visualized using a Zeiss Axiovert or LSM 510 Meta (Carl Zeiss). For SA:V calculations, LSM Image Examiner software was used. Briefly, the apical and basolateral outlines were drawn, and the length of the apical membrane outline was divided by the area between the apical and basolateral outlines. To determine the approximate volume (V) of 2D cells on a thin layer of lrBM, the maximum cross-sectional height (h) of a confluent region was multiplied by the length (l) and width (w) of the region. The SA:V ratio was taken as the inverse of h, since $SA = l \times w$ and $V = h \times l \times w$, so SA:V would be $(l \times w)/h \times (l \times w)$, or $1/h$.

Primary Mouse Mammary Epithelial Cells (MMEC). MMEC were isolated from CD1 mice, as described in ref. 15. Cells were cultured as monolayers on plastic or a thin layer of lrBM (Growth-factor Reduced Matrigel, BD Biosciences), or as 3-D mammospheres within a slab of lrBM. Cells were cultured in DMEM/F12 with 5% FBS, insulin (5μg/ml), and hydrocortisone (0.5μg/ml) (Lonza), with or without 5μg/ml purified prolactin (Sigma). Hyposmotic treatment (50%) consisted of media diluted with an equal volume of distilled water prior to the addition of hormones. PMCA2 mRNA was quantified by multiplex TaqMan QRT-PCR (Assays On-Demand, Applied Biosystems). The PMCA2 (*Atp2b2*) assay, Mm437640_m1 (FAM), and the endogenous control, *Gapd*, Mm99999915_g1 (VIC) were used with One-Step QRT-PCR/Platinum Taq (Invitrogen).

Overexpression of PMCA2 in T47D Cells. Mouse PMCA2b/w was cloned by RT-PCR from lactating CD1 mouse mammary tissue. cDNA was made using the ProtoScript AMV First Strand cDNA Synthesis Kit (NEB), and PMCA2b/w was amplified with the Phusion High Fidelity PCR Kit (NEB) using the primers: 5′-CA CCA GCA AAC ATG GGT GAC ATG A-3′ and 5′-AGC TAA AGC GAC GTC TCC AG-3′. The sequence of PMCA2 cDNA cloned from lactating mouse mammary gland was deposited in GenBank (accession no. GU734816). T47D cells (ATCC) were transfected with a PMCA2b/w-containing vector or empty vector (pT-REx-DEST30) and selected in 500μg/ml G418 (Invitrogen). Calpain activity was measured using the Calpain Activity Assay Kit (BioVision). Prior to lysis, mammary glands were minced and washed in PBS with protease inhibitor cocktail (Roche) until milk was completely removed.

Tissue Microarray Analysis and Statistical Methods. The patient cohort consisted of 652 primary breast cancer specimens retrospectively obtained from 1953 to 1983 (Table S1). Clinicopathologic data were extracted from Yale and Connecticut Tumor Registries, in accordance with the Yale Human Investigations Committee. TMA slides were stained as previously described (2). The primary antibodies were rabbit anti-PMCA2 (Affinity BioReagents) and a mouse anti-cytokeratin (DAKO) to distinguish the tumor from stroma. Automated image acquisition and analysis (AQUA) have been described previously (2). The AQUA score is proportional to cellular PMCA2 concentration averaged across the entire region of the tumor, defined by cytokeratin.

Prism 5.02 for Windows (GraphPad) was used for all statistical analyses, except for Oncomine and breast cancer TMA analyses. Student's t test was used for comparisons between two groups, while one-way ANOVA was used for multiple comparisons. The posttests employed with one-way ANOVA included the test for linear trend between mean and column number and the Newman–Keuls multiple comparisons test. Oncomine data and statistics are from www.oncomine.org (3). For the breast cancer tissue microarray, data analysis was performed using StatView. Cox proportional hazards model was used to access prognostic significance with overall survival as well as multivariate analysis of markers using 20-year survival time period. Survival curves were made using the Kaplan–Meier method. Unpaired t test analysis was used to examine the associations between PMCA2 with clinical variables. For all analyses, $P < 0.05$ was considered statistically significant.

1. VanHouten JN, Neville MC, Wysolmerski JJ (2007) The calcium-sensing receptor regulates plasma membrane calcium adenosine triphosphatase isoform 2 activity in mammary epithelial cells: A mechanism for calcium-regulated calcium transport into milk. *Endocrinology* 148:5943–5954.
2. Camp RL, Chung GG, Rimm DL (2002) Automated subcellular localization and quantification of protein expression in tissue microarrays. *Nat Med* 8:1323–1327.
3. Rhodes DR, et al. (2004) ONCOMINE: A cancer microarray database and integrated data-mining platform. *Neoplasia* 6:1–6.

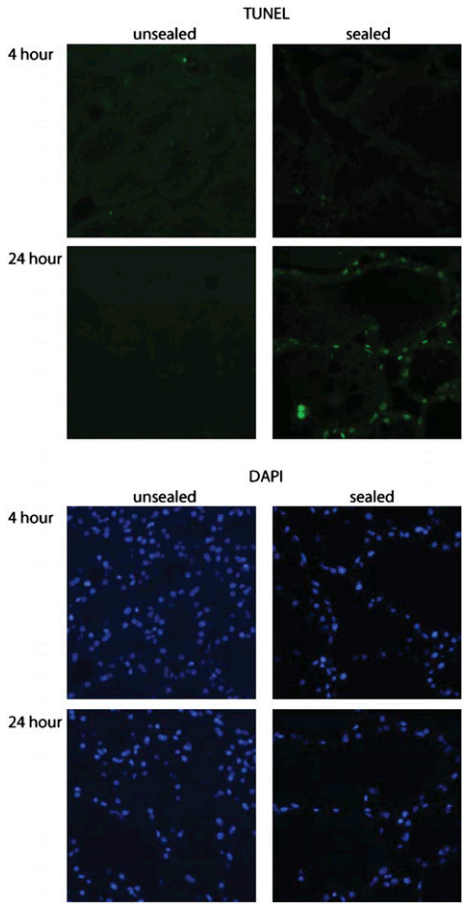

Fig. S1. Mammary epithelial cell apoptosis in the teat-sealing model of mammary gland involution. Mammary glands were analyzed for apoptosis by TUNEL staining at 4 and 24 h after teat canals were sealed. The contralateral unsealed glands served as controls. TUNEL-positive nuclei (green) were absent from unsealed mammary glands, and were apparent only after 24 h in the sealed mammary glands. Nuclei were counter stained with DAPI (blue).

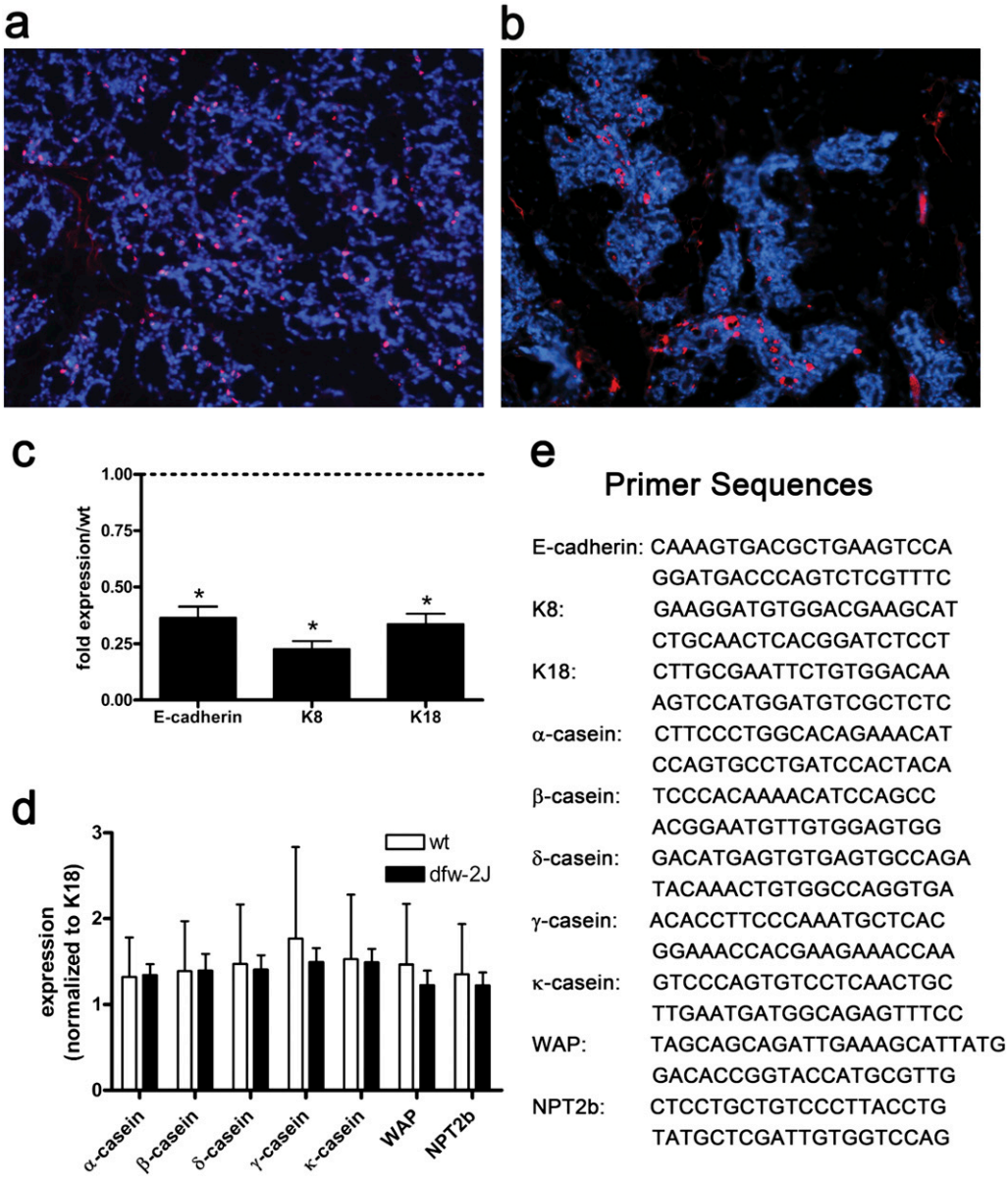

Fig. S2. PMCA2 is not necessary for proliferation or differentiation of mammary epithelial cells. Pregnant (P18) WT (*A*) or dfw-2J (*B*) mice were injected with 50 mg/kg BrdU, and mammary tissue was harvested after a labeling interval of 2.5 h. Tissue was fixed for 12 h in methacarn, and sections were stained with fluorescein-anti-BrdU (Zymed) and DAPI. Three WT and 3 dfw-2J mice were analyzed. The proliferative index (mean ± SEM) was 9.92 ± 1.5% for WT (401 nuclei from five fields counted) and 8.47 ± 2.71% for dfw-2J (302 nuclei from five fields counted; $P = 0.5865$ by *t* test). MEC content was reduced, as shown by the markers E-cadherin, keratin-8 (K8), and keratin-18 (K18), which were significantly lower in dfw-2J mammary glands ($n = 4$, $P = 0.0009$, 0.0002, and 0.0007, respectively, by one-sample *t* test), relative to WT glands by SYBR-green qRT-PCR (*C*). When corrected for cell number (K18 expression), there was no difference in the differentiation of dfw-2J mammary glands, as measured by SYBR-green qRT-PCR (*D*) for α-, β-, δ-, γ-, and κ-casein, whey acidic protein (WAP), or the sodium-phosphate cotransporter 2b (NPT2b). Bars in *C* and *D* represent the mean ± SEM. qRT-PCR primer sequences are shown in *E*.

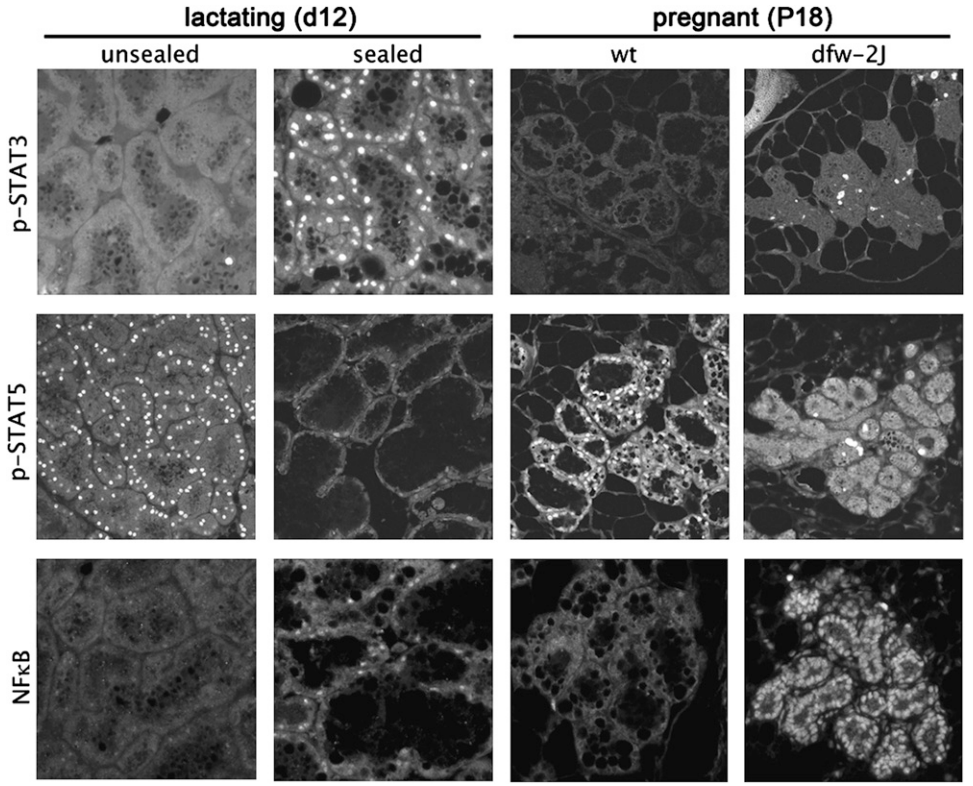

Fig. S3. PMCA2-deficient apoptotic mammary glands resemble early mammary gland involution. Shown is the comparison of lactating (unsealed) and involuting (sealed) glands in WT mice and WT and dfw-2J glands at the end of pregnancy (P18). The early stage of mammary gland involution (sealed) is characterized by increased nuclear phospho-STAT3 (p-STAT3), decreased nuclear phospho-STAT5 (p-STAT5), and activation of NFκB, compared with the noninvoluting, lactating mammary gland (unsealed). The WT gland at P18 resembles the lactating gland, with low levels of nuclear p-STAT3 and NFκB and high levels of p-STAT5. Similar to the involuting mammary gland (sealed), the dfw-2J gland during pregnancy (P18) showed an increase in p-STAT3 and nuclear NFκB, with loss of p-STAT5. Staining was performed on sections from at least two animals per group.

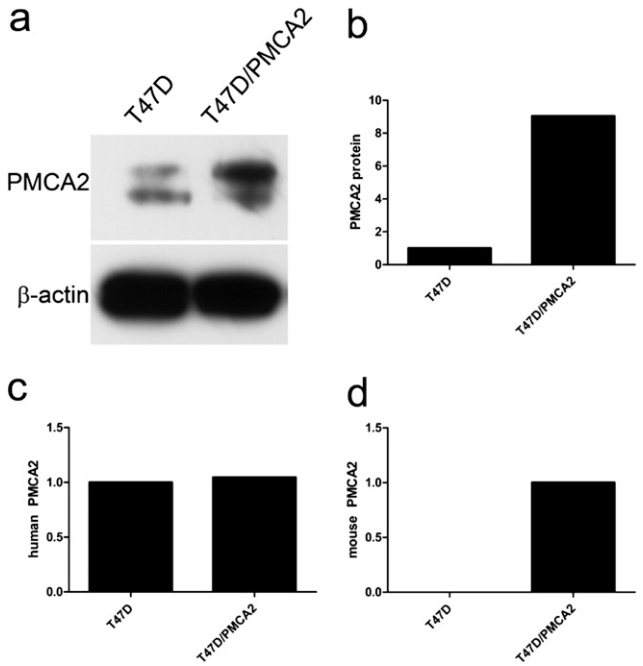

Fig. S4. Expression of mouse mammary PMCA2 in T47D breast cancer cells. Western blotting (*A*) and multiplex TaqMan qRT-PCR (*C* and *D*) confirmed the overexpression of mouse mammary PMCA2 in transfected T47D/PMCA2 cells, relative to empty-vector-transfected control T47D cells (also called T47D/EV cells). Quantitation of the Western blot showed a ninefold higher expression of PMCA2 protein in membrane extracts from T47D/PMCA2 cells, compared with T47D (T47D/EV) cells (*B*). Although the expression of human PMCA2 mRNA (*ATP2B2*) was the same in both cell types (*C*), mouse PMCA2 mRNA (*Atp2b2*) was readily detectable in T47D/PMCA2 cells (*D*) but essentially undetectable in T47D control (T47D/EV) cells.

Table S1. Characteristics of the entire TMA patient cohort (*n* = 652) and of only those patients <50 y old (*n* = 171)

	All patients *N* (%)	Patients <50 y old *N* (%)
Age (y)		
<50	171 (26)	
≥50	466 (72)	
Not specified	15 (2)	
Histology		
Infiltrating duct	510 (78)	125 (73)
Carcinoma NOS	114 (18)	33 (19)
Other	28 (4)	13 (8)
Tumor size (cm)		
<2	210 (32)	49 (29)
≥2, <5	280 (43)	72 (42)
≥5	101 (16)	30 (18)
Not specified	61 (9)	20 (11)
Nodal status	319 (49)	92 (54)
Positive		
Negative	320 (49)	79 (46)
Not available	13 (2)	0 (0)
Nuclear grade	113 (17)	23 (14)
1		
2	310 (48)	74 (43)
3	169 (26)	56 (33)
Not specified	60 (9)	18 (10)
ER	321 (49)	53 (31)
Positive		
Negative	287 (44)	108 (63)
Not available	44 (7)	10 (6)
PR	296 (45)	73 (43)
Positive		
Negative	293 (45)	82 (48)
Not available	63 (10)	16 (9)
HER2	374 (57)	96 (56)
0		
1	116 (18)	27 (16)
2	40 (6)	10 (6)
3	67 (10)	26 (15)
Not specified	55 (8)	12 (7)
Follow-up (y) [median (range)]	12.53 (0.19–53.9)	18.9 (0.20–53.9)

Table S2. Correlation of continuous PMCA2 AQUA scores with clinicopathologic markers by unpaired *t* tests

Variable	Number of patients*	AQUA PMCA2 (SD)	*P* value
Tumor size			
Less than 2	177	33.567 (12.777)	0.0575
2 or greater	323	35.572 (10.335)	
Age			
Younger than 50	141	34.643 (10.385)	0.6463
50 or older	394	35.154 (11.658)	
Nuclear grade			
Low grade	352	34.318 (11.217)	0.0142
High grade	148	37.056 (11.666)	
Nodal status			
Node negative	272	33.319 (10.771)	0.0007
Node positive	265	36.596 (11.391)	
ER status			
ER negative	235	35.229 (11.366)	0.7191
ER positive	283	34.870 (11.264)	
PR status			
PR negative	240	35.901 (11.794)	0.1424
PR positive	265	34.402 (11.137)	
HER2 status			
HER2 negative	415	34.219 (10.031)	<0.0001
HER2 positive	98	39.365 (14.904)	

*Total number in cohort is 652 however, the number of patients represented are those with evaluable PMCA2 scores and recorded variables (e.g., tumor size).

Table S3. Correlation of clinicopathologic markers with cancer-specific survival in the entire TMA cohort

Variables	*P* value	Relative risk	95% CI
Tumor size			
2 or greater	$P < 0.0001$	1.949	1.473–2.577
Age			
50 or greater	$P = 0.0646$	1.297	0.984–1.706
Nuclear grade			
High grade	$P = 0.0018$	1.511	1.166–1.967
Nodal status			
Node positive	$P < 0.0001$	2.404	1.879–3.077
ER status			
ER negative (0 vs. 1,2,3)	$P = 0.0273$	1.362	1.032–1.704
PR status			
PR negative (0 vs. 1,2,3)	$P = 0.0033$	1.472	1.137–1.905
HER2 status			
HER2 positive (0,1,2 vs. 3)	$P = 0.2238$	1.209	0.890–1.642
PMCA2			
Continuous scores	$P = 0.0089$	1.014	1.003–1.024

Table S4. Multivariate analysis of survival with clinicopathologic markers and PMCA2 in the entire TMA cohort

Variables	*P* value	Relative risk	95% CI
Tumor size			
2 or greater	$P = 0.0003$	1.831	1.318–2.542
Nuclear grade			
High grade	$P = 0.1736$	1.241	0.909–1.695
Nodal status			
Node positives	$P < 0.0001$	1.976	1.453–2.688
ER status			
ER negative	$P = 0.2308$	1.203	0.889–1.628
PR status			
PR negative	$P = 0.7439$	1.051	0.778–1.421
PMCA2			
Continuous scores	$P = 0.0489$	1.013	1.000–1.025